Development of a pseudo-uniform structural quantity for use in active structural acoustic control of simply supported plates: An analytical comparison

Jeffery M. Fisher and Jonathan D. Blotter[a)]
Department of Mechanical Engineering, Brigham Young University, Provo, Utah 84602

Scott D. Sommerfeldt and Kent L. Gee
Department of Physics and Astronomy, Brigham Young University, Provo, Utah 84602

Active structural acoustic control has been an area of research and development for over two decades with an interest in searching for an "optimal" error quantity. Current error quantities typically require the use of either a large number of transducers distributed across the entire structure, or a distributed shaped sensor, such as polyvinylidene difluoride. The purpose of this paper is to investigate a control objective function for flat, simply-supported plates that is based on transverse and angular velocity components combined into a single composite structural velocity quantity, termed V_{comp}. Although multiple transducers are used, they are concentrated at a single location to eliminate the need for transducers spanning most or all of the structure. When used as the objective function in an active control situation, squared V_{comp} attenuates the acoustic radiation over a large range of frequencies. The control of squared V_{comp} is compared to other objective functions including squared velocity, volume velocity, and acoustic energy density. The analysis presented indicates that benefits of this objective function include control of radiation from numerous structural modes, control largely independent of sensor location, and need to measure V_{comp} at a single location and not distributed measurements across the entire structure. © *2012 Acoustical Society of America.* [http://dx.doi.org/10.1121/1.3699264]

I. INTRODUCTION

Active structural acoustic control (ASAC) is a form of active control which focuses on the control of structural vibrations in a manner that minimizes acoustic radiation from a structure. Typically, force actuators are applied directly to the structure to control vibration of that structure. The benefits of ASAC over traditional sound field control using a speaker arrangement are associated with the control of sound at the source and the system compactness. Structurally applied actuators are much less intrusive than speakers because they do not use space in the acoustic field, which in some cases can be very valuable, such as in confined cabins.[1]

While the compactness of an ASAC system is beneficial, problems exhibited in the active control of a sound field are also present in vibration control. These include issues such as sensor and actuator selection and placement, as well as the selection of the appropriate control objective function. As mentioned by Sommerfeldt and Nashif,[2] the optimal placement of the sensor(s) is a function of the control objective function so the challenges become intertwined. In the case of enclosed sound fields, using acoustic energy density as an objective function resolved many of the problems introduced by using squared pressure. While squared pressure works well to attenuate the sound field in areas directly surrounding the microphone(s), other areas might see an

increase in noise level. Acoustic energy density has become a common objective function because it can generally produce a more global effect.[2] Another benefit of acoustic energy density lies in the increased flexibility of sensor placement. In modal fields where the squared pressure approaches zero at nodal locations, energy density usually does not because of its dependence on both particle velocity and pressure. Thus, an energy density-based objective function can be more desirable than one based on squared pressure. An easy example to illustrate this point is pressure control in the sound field. While acoustic energy density has proven successful in active noise control (ANC), the quantity deals with acoustic variables and not surface vibrations. The challenge associated with ASAC is that an objective function with the robustness of acoustic energy density does not yet exist.

The objective functions mentioned above all deal with the acoustic field generated by a vibrating structure or noise source. Although these objective functions deal with the acoustic field, in ASAC the control actuators are applied to the structure so as to control the structural vibrations in a manner that reduces the acoustic objective function. This has proven effective in many situations which include controlling pressure.[3–5] However, the current interest is to determine a structural objective function that will perform similarly to the acoustic energy density objective function. The result would be a control scheme with an objective function that requires a small, closely spaced array of structural sensors placed on the structure in a single relatively arbitrary

[a)]Author to whom correspondence should be addressed. Electronic mail: jblotter@byu.edu

location. Although there would still be multiple sensors, they would be closely spaced in a fixed position array at a single location on the structure and not distributed across the entire domain.

A significant issue in ASAC is in determining which objective function on the structure will provide the best global acoustic attenuation. It has been shown that simply minimizing the vibration does not necessarily decrease the acoustic radiation.[6] There are two main mechanisms of ASAC, as explained by Snyder and Hansen.[7] One way is to increase the impedance of the structural modes, thus decreasing their amplitude. This technique is known as modal control. The second method is to alter the amplitudes and phases of the same structural modes. This is known as modal rearrangement. The purpose of modal rearrangement is either to reduce the overall vibration level of the structure or to create vibration patterns which radiate less efficiently. Portions of both modal control and rearrangement can be seen in different control situations, and each does not have to be the only method of control.

Certain energy-based structural metrics and their relationship to acoustic radiation have been previously investigated. Elliot *et al.*[8,9] investigated the effect of sensing[10] and controlling volume velocity, but this has proven to be somewhat ineffective at higher frequencies because the number of sensors required for reasonable attenuation, in many situations, is too many for practical purposes.[11–17] Another quantity which has been investigated is structural intensity, or structural power flow. However, it has been shown that structural power flow has little effect on acoustic intensity[18] and thus shows little promise as a control metric. The control of acoustic radiation modes using structural sensors has shown promise, but requires the use of multiple sensors and knowledge of the radiation modes that contribute significantly to the overall radiation.[19–21]

The remainder of this article discusses analytical investigations of a new objective function for flat plates that is based on measurement of transverse and angular velocity components. These components are combined into a single objective function which has been called the composite velocity, or V_{comp}. The benefits of this objective function include control of radiation from numerous structural modes, control largely independent of sensor location, and need to only measure V_{comp} at a single location. While ongoing efforts may extend these concepts to general structures, the focus of this article is on simply supported plates.

In this article, Sec. II presents the development of the V_{comp} objective function. Section III presents analytical results and compares the results to other control strategies. Conclusions and a discussion of directions for future work are then presented in Sec. IV.

II. DEVELOPMENT OF COMPOSITE VELOCITY

A. Structural acoustic relationships

There are two relatively well known and accepted relationships between structural vibrations and acoustic radiation. The first of these is the concept of volume velocity. Research has suggested that much of the acoustic radiation

from a structure is attributed to volume velocity.[8,9,20,22] This can be viewed from Rayleigh's integral, which is given as

$$P(\mathbf{r}, t) = \frac{j\omega\rho_o}{2\pi} e^{j\omega t} \int_S \frac{\tilde{v}_n(\mathbf{r}_s)e^{-jkR}}{R} dS, \tag{1}$$

where P is the pressure, ω is the angular frequency in radians per second, and ρ_o is the density of the medium through which the sound is propagating. Also, $\mathbf{r}$ is the position vector of the observation point, $\mathbf{r_s}$ is the position on the surface having velocity amplitude $\tilde{v}_n$, and R is the magnitude of $\mathbf{r}$–$\mathbf{r}_s$. As can be seen, a reduction of $\tilde{v}_n$ on the structure will tend to decrease the pressure at all points in the field. Volume velocity by definition refers to the rate of displacement of fluid volume.[23] Thus, although in some instances the amplitude of the localized vibration response may be large, the volume velocity can be close to zero. As research has shown, odd modes radiate more efficiently than even modes because they have non-zero volume velocity. This is one of the reasons that volume velocity has been strongly associated with acoustic radiation.

A second relationship between structural vibrations and acoustic radiation deals with acoustic radiation modes. As explained by Fahy and Gardonio,[23] these are modes which radiate independent of the structural vibrations. The derivation given in this paper follows the elementary radiator formulation described by Elliot and Johnson.[20] Using this method, a panel is divided into a grid of N elements whose transverse velocities are given by $\tilde{v}_{er}$. The complete vibration of the panel can be represented by the vector

$$\{\tilde{v}_e\} = [\tilde{v}_{e1}\tilde{v}_{e2} \ldots \tilde{v}_{eN}]^T. \tag{2}$$

Using this, the total radiated sound power is given by

$$\overline{P}(\omega) = \{\tilde{v}_e\}^T [R_R]\{\tilde{v}_e\}. \tag{3}$$

The matrix $[R_R]$ is defined as the radiation resistance matrix and is given by

$$[R_R] = \frac{\omega^2 \rho_o A_e^2}{4\pi c} \begin{bmatrix} 1 & \frac{\sin(kD_{12})}{kD_{12}} & \cdots & \frac{\sin(kD_{1N})}{kD_{1N}} \\ \frac{\sin(kD_{21})}{kD_{21}} & 1 & \cdots & \vdots \\ \cdots & \cdots & \ddots & \vdots \\ \frac{\sin(kD_{N1})}{kD_{N1}} & \cdots & \cdots & 1 \end{bmatrix}, \tag{4}$$

where A_e is the cross-sectional area of each individual element, D_{ij} is the distance between the ith and jth elements, ρ_0 is the density of air, c is the speed of sound in air, and k is the wavenumber. The matrix $[R_R]$ is a positive definite matrix. Given the $[R_R]$ matrix, the acoustic radiation modes are obtained from the orthogonal decomposition of this matrix

$$[R_R] = [Q]^T [\Lambda][Q], \tag{5}$$

where $[Q]$ is a matrix of orthogonal eigenvectors and $[\Lambda]$ is a diagonal matrix of eigenvalues. The relative magnitudes of

the radiation modes are given by the elements of $[\Lambda]$, and the shape of each radiation mode is given by the corresponding row of $[Q]$.

The general shapes of the first six acoustic radiation modes of a plate that is simply supported on all four sides are shown in Fig. 1. It can be observed that the volume velocity for the structure is closely related to the first acoustic radiation mode. The overall power radiated is given by

$$\overline{P}(\omega) = \{\tilde{y}\}^H[\Lambda]\{\tilde{y}\} = \sum_{r=1}^{N} \lambda_r |\tilde{y}_r|^2, \tag{6}$$

where

$$\{\tilde{y}\} = [Q]\{\tilde{v}_e\}. \tag{7}$$

Here, N is the total number of elements. λ_r and $\tilde{y}_r$ are the components corresponding to the radiation mode of interest. The shape of each radiation mode is mildly dependent on frequency. The higher the frequency, the more curvature appears in the individual radiation modes. In order to compare the relative importance of the individual radiation modes, the power radiated by the individual acoustic radiation modes, as given by the individual terms in Eq. (6), can be compared.

Controlling radiation modes has been an effective way to control the power radiated from a panel. However, the structural geometry associated with the vibrations must be known *a priori* to calculate the radiation modes and determine sensor locations that are conducive to sensing all significant radiation modes present. In most cases, structural vibrations cannot be fully mapped without equipment such as multiple accelerometer arrays, film sensors, or a scanning laser Doppler vibrometer, and the radiation modes cannot be obtained without some numerical analysis of the structure.
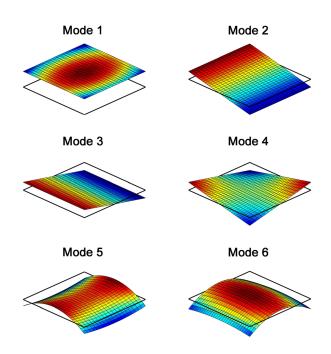
B. Composite velocity derivation

The previous analysis of both volume velocity and acoustic radiation modes suggests advantages and disadvantages of both approaches. Volume velocity is generally more straightforward to sense but the radiation modes can better capture the total acoustic radiation. However, it is generally more involved to measure multiple radiation modes. What is sought is a measurement that is more straightforward, which can also capture the radiation contributions associated with the radiation modes. If this new quantity could be created using multiple sensors coupled together acting much like a point sensor and placed at a single location on the structure rather than as a large distributed array of sensors, a global result could potentially be achieved using a more compact sensor configuration than required for the other objective functions. In other words, this would represent a relatively local measurement that provides some measure of the global radiation properties of the structure.

A quantity that strives to mimic the contributions of the acoustic radiation modes has been developed. This quantity, termed V_{comp} for composite velocity, takes multiple velocity components measured at the same location on the structure and combines them into a single quantity. The idea is to represent all of these velocity components of the structure in one single equation. The square of V_{comp} is then used as the objective function in an active control system, in order to provide an objective function that is a quadratic function of the control filter coefficients.

To develop the concept of V_{comp}, an analytical model of a simply supported, damped plate with multiple point force locations has been used. The extension of these concepts to general and more complex structures is not presented here but is the focus of ongoing research.

The transverse displacement of the plate is given by Eqs. (8)–(11)

$$w(x, y) = \sum_{q=1}^{F} \frac{f_q}{\rho_s h}$$
$$\times \sum_{m}^{\infty} \sum_{n}^{\infty} \frac{W_{mn}(x,y)W_{mn}(x_q,y_q)\left[\omega_{mn}^2 - \omega^2 - j\eta\omega_{mn}^2\right]}{\left[\omega_{mn}^2 - \omega^2\right]^2 + \eta^2\omega_{mn}^4}, \tag{8}$$

where

FIG. 1. (Color online) Acoustic radiation mode shapes.

TABLE I. Properties of the simply supported plate.

Property	Value
Length (x direction) (L_x)	0.483 m
Length (y direction) (L_y)	0.762 m
Thickness (h)	0.001 m
Young's modulus (E)	207×10^9 Pa
Poisson's ratio (ν)	0.29
Density (ρ)	7800 kg/m^3
Damping ratio (η)	0.1%

J. Acoust. Soc. Am., Vol. 131, No. 5, May 2012

J. M. Fisher *et al.*: Structural objective function   3835

TABLE II. First 15 resonance frequencies of the rectangular plate.

Mode	Modal frequency Hz
(1,1)	13.4
(2,1)	24.9
(1,2)	42.1
(3,1)	44.1
(2,2)	53.6
(4,1)	70.9
(3,2)	72.7
(1,3)	89.8
(4,2)	99.6
(2,3)	101.3
(5,1)	105.4
(3,3)	120.5
(5,2)	134.1
(4,3)	147.3
(6,1)	147.6

FIG. 2. (Color online) Structural quantities used to create squared V_{comp}.

$$W_{mn}(x,y) = \frac{2}{\sqrt{L_x L_y}} \sin\left(\frac{m\pi x}{L_x}\right) \sin\left(\frac{n\pi y}{L_y}\right), \tag{9}$$

$$\omega_{mn} = \sqrt{\frac{D}{\rho_s h}\left(\frac{m^2\pi^2}{L_x^2} + \frac{n^2\pi^2}{L_y^2}\right)}, \tag{10}$$

$$D = \frac{Eh^3}{12(1-v^2)}. \tag{11}$$

Here f_q is the amplitude of the qth driving force, ρ_s is the density of the plate material, E is Young's modulus, v is Poisson's ratio, h is the plate thickness, and L_x and L_y are the plate dimensions. The structural damping ratio is given by η, ω is the driving frequency in radians per second, and m and n are structural mode shape numbers. The plate properties used are given in Table I and the first 15 resonance frequencies
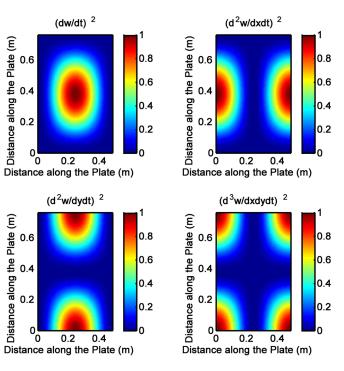
associated with the structural modes of the plate, as computed by Eq. (10), are given in Table II.

For the (1,1) mode of the plate excited by a single point force at an anti-node, four velocity terms were computed. These correspond to transverse, rocking, and twisting velocities, given by

$$\left(\frac{dw}{dt}\right), \left(\frac{d^2w}{dxdt}\right), \left(\frac{d^2w}{dydt}\right), \left(\frac{d^2w}{dxdydt}\right), \tag{12}$$

and normalized plots of these quantities are given in Fig. 2. Equations for these four terms are given as

$$\frac{dw}{dt}(x,y) = \sum_{q=1}^{F} \frac{f_q}{\rho_s h} \sum_{m}^{\infty} \sum_{n}^{\infty} \frac{W_{mn}(x,y) W_{mn}(x_q, y_q)\left[\omega_{mn}^2 - \omega^2 - j\eta\omega_{mn}^2\right]}{\left[\omega_{mn}^2 - \omega^2\right]^2 + \eta^2\omega_{mn}^4} j\omega, \tag{13}$$

$$\frac{d^2w}{dxdt}(x,y) = \sum_{q=1}^{F} \frac{f_q}{\rho_s h} \sum_{m}^{\infty} \sum_{n}^{\infty} \frac{\frac{2}{\sqrt{L_x L_y}}\cos\left(\frac{m\pi x}{L_x}\right)\sin\left(\frac{n\pi y}{L_y}\right) W_{mn}(x_q, y_q)\left[\omega_{mn}^2 - \omega^2 - j\eta\omega_{mn}^2\right]}{\left[\omega_{mn}^2 - \omega^2\right]^2 + \eta^2\omega_{mn}^4} \left(\frac{m\pi}{L_x}\right) j\omega, \tag{14}$$

$$\frac{d^2w}{dydt}(x,y) = \sum_{q=1}^{F} \frac{f_q}{\rho_s h} \sum_{m}^{\infty} \sum_{n}^{\infty} \frac{\frac{2}{\sqrt{L_x L_y}}\sin\left(\frac{m\pi x}{L_x}\right)\cos\left(\frac{n\pi y}{L_y}\right) W_{mn}(x_q, y_q)\left[\omega_{mn}^2 - \omega^2 - j\eta\omega_{mn}^2\right]}{\left[\omega_{mn}^2 - \omega^2\right]^2 + \eta^2\omega_{mn}^4} \left(\frac{n\pi}{L_x}\right) j\omega, \tag{15}$$

$$\frac{d^3w}{dydydt}(x,y) = \sum_{q=1}^{F} \frac{f_q}{\rho_s h} \sum_{m}^{\infty} \sum_{n}^{\infty} \frac{\frac{2}{\sqrt{L_x L_y}}\cos\left(\frac{m\pi x}{L_x}\right)\cos\left(\frac{n\pi y}{L_y}\right) W_{mn}(x_q, y_q)\left[\omega_{mn}^2 - \omega^2 - j\eta\omega_{mn}^2\right]}{\left[\omega_{mn}^2 - \omega^2\right]^2 + \eta^2\omega_{mn}^4} \left(\frac{m\pi}{L_x}\frac{n\pi}{L_y}\right) j\omega. \tag{16}$$

TABLE III. Structural quantity scaling factors to create a uniform value.

Quantity	$\dfrac{dw}{dt}$	$\dfrac{d^2w}{dxdt}$	$\dfrac{d^2w}{dxdt}$	$\dfrac{d^2w}{dxdt}$
Factor	$\alpha = 1$	$\beta = \left(\dfrac{L_x}{m\pi}\right)^2$	$\gamma = \left(\dfrac{L_y}{n\pi}\right)^2$	$\delta = \left(\dfrac{L_xL_y}{mn\pi^2}\right)^2$
Avg. value	1.0	0.01211	0.01717	1.8654×10^{-4}

Considering these four velocity terms and referring to Fig. 2, each of the four terms is dominant in a different spatial portion of the plate. With a combination of these terms, it was determined that a fairly uniform velocity field can be developed. Furthermore, comparing these four quantities to the first four acoustic radiation modes given in Fig. 1, a commonality can be observed. The first radiation mode can be viewed as a transverse velocity, the second a rocking velocity in x, the third a rocking velocity in y, and the fourth, a twisting velocity. In order to create a uniform field over the entire plate, a simple linear combination of these quantities was investigated as given by

$$\left(V_{\text{comp}}\right)^2 = \alpha\left(\frac{dw}{dt}\right)^2 + \beta\left(\frac{d^2w}{dxdt}\right)^2 + \gamma\left(\frac{d^2w}{dydt}\right)^2 + \delta\left(\frac{d^3w}{dxdydt}\right)^2. \tag{17}$$

As can be seen by Eqs. (13)–(16), the maximum values of each term in Eq. (17) will vary with a standard scaling value which is based on the size of the plate as well as the structural mode at which the plate is vibrating. Table III defines the α, β, γ, and δ standard scaling values for each of the terms, which when multiplied by the associated quantity will create a maximum value equal to that of the transverse velocity. There is one independent variable, which is taken to be α. Using this value, the other parameters are then determined. Values for α, β, γ, and δ, with an arbitrary α value, can be computed for any structural mode (m, n) and plate dimensions. Using these scaling value definitions with the plate parameters listed in Table I, the analytically computed squared V_{comp} for the $(1, 1)$ structural mode has a uniform value over the entire plate with an error of less than $\pm 0.01\%$.

It will also be shown that average α, β, γ, and δ values can be computed and provide very good results. In this work, the average α, β, γ, and δ values were computed by averaging the individual values over the 15 frequencies corresponding to the mode shapes from 0–150 Hz as shown in Table II. These average values are also presented in Table III.

TABLE IV. Force actuator locations.

Actuator/Sensor	Location (x, y)
Primary disturbance force	$(0.083, 0.629)$
Control force	$(0.083, 0.127)$

TABLE V. Sensor locations.

Property	Location	Arena
V_{comp}	$(0.286, 0.432)$	Plate
Point velocity	$(0.286, 0.432)$	Plate
Volume velocity	(6 evenly spaced sensors in x, 10 evenly spaced sensors in y)	Plate
Acoustic energy density	$(1.0, 1.0, 1.0)$	Room

III. ACOUSTIC RADIATION

A. Radiated power comparison

In order to compare levels of acoustic radiation, the radiated power was chosen as the benchmark and was calculated using the elementary radiator method given by Johnson and Elliot.[20] As stated, this method involves breaking the structure into a spatial grid of small acoustic radiators. The power radiated from a plate using elementary radiators is given by Eq. (3), where $\{\tilde{v}_e\}$ is a velocity vector containing the velocities of the individual elements and $[R]$ is the radiation resistance matrix solved for in Sec. II A.

Using the analytical model presented in Sec. II B, a primary force location, control force location, and a sensor location were chosen. The locations of the actuators are given in Table IV, with the sensor location to be given later.

With the objective function chosen as the square of V_{comp}, the optimal magnitude and phase of the control force were determined by using a simple gradient-based algorithm, which minimized the objective function at the error sensor location. As a constraint on the gradient-based algorithm, the amplitude of the control force was limited to five times the amplitude of the primary disturbance force. Once the controlled velocity field was established, the radiated powers from both the controlled and uncontrolled cases were compared.

For comparison, squared velocity at the sensor location, estimated volume velocity, and acoustic energy density were also used as objective functions. An approximation was used for the volume velocity where the number of points used to acquire a good estimate of the volume velocity was based on work by Sors and Elliott[8] and is given by
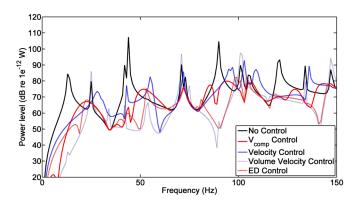

FIG. 3. (Color online) Analytical radiated power vs objective function.

TABLE VI. Average attenuation vs objective function.

Control	Average attenuation (dB)
Squared V_{comp}	5.8
Squared velocity	2.7
Volume velocity	12.4
Acoustic energy density	8.6

$$N = \frac{5}{3\pi} c_o l \sqrt{\frac{m}{D}}, \qquad (18)$$

where c_o is the speed of sound in the fluid, m is the mass per unit area, D is the bending stiffness, and l is the smallest plate dimension. For this specific case, the approximate number of sensors is 62. This number is not practical for experimental purposes. However, 60 points were used for this analytical study with 10 equally distributed sensors in the y-direction and 6 in the x-direction. In the case of acoustic energy density control, the plate was placed on the wall of a room with dimensions $5.70 \times 2.50 \times 4.30$ m^3. The plate was placed near the center of the wall with dimensions 5.70×2.50 m^2, with the offset from the corner of the room to the lower left corner of the plate being 2.59×0.89 m^2. The locations of the error sensors, with their respective objective functions, are given in Table V.

The radiated power at frequencies spanning the first 15 structural modes can be seen in Fig. 3. Both the uncontrolled radiated power and the radiated power after control using the four objective functions are shown. The average attenuations over the frequency range from 0–150 Hz for each of the four cases is obtained by integrating the total power over this frequency range, with and without control. Those average attenuations, expressed in dB, are given in Table VI.

When comparing these attenuations, volume velocity does considerably better, but considering the number of sensors involved, it is less practical in implementation. Also, an important note is that the maximum increase in radiated power is less for V_{comp} control than for any other investigated control scheme. This is an important consideration for cases where the structural excitation is narrowband in nature. For those cases, it is possible that implementation of active control could increase the radiation for some frequencies of excitation, and it is desired to minimize those possible undesired amplifications. Thus, having a small maximum increase in radiated power is a desirable feature of an effective active control scheme. The maximum and minimum attenuations for each of the control cases are given in Table VII.

TABLE VII. Maximum and minimum attenuation vs objective function.

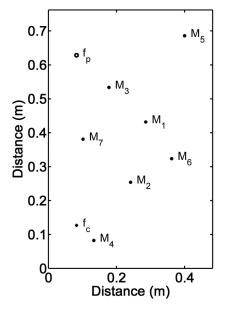| Control	Largest attenuation (dB)	Largest increase (dB)
Squared V_{comp}	43.5	6.3
Squared velocity	40.0	15.6
Volume velocity	57.5	13.5
Acoustic energy density	54.4	7.6

FIG. 4. Force actuator and sensor positions.

Even though volume velocity control produced a larger attenuation, the maximum increase in radiated power is more than when minimizing squared V_{comp} and again, uses considerably more measurement sensors, approximately 15 times the amount needed for squared V_{comp}. In comparing squared V_{comp} control to acoustic energy density, squared V_{comp} attenuates the radiated power by a few decibels less overall. However, considering the fact that sensors can be integrated or placed on the structure in a minimum number of locations, and are not needed in the sound field, the loss in control may be worth more efficient implementation, making it a potentially beneficial structural objective function. As can be observed in the results, controlling the quantity squared V_{comp} nearly always decreased the radiated power, attenuated all of the resonance peaks by at least 5 dB, and produced an overall reduction of almost 6 dB.

B. Sensor placement

A major benefit of controlling squared V_{comp} is that the control performance is largely independent of sensor location. To illustrate this, the sensor was moved to multiple locations on the plate with comparable results at almost all locations. Other plate locations are given in Fig. 4 with the corresponding radiated power at each location given in

TABLE VIII. Average attenuation using squared V_{comp} vs measurement position.

Measurement position	Average attenuation (dB)
M_1	5.8
M_2	4.6
M_3	4.2
M_4	2.5
M_5	2.4
M_6	4.9
M_7	4.8

J. M. Fisher *et al.*: Structural objective function

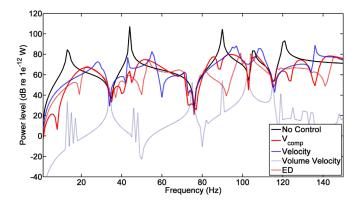FIG. 5. (Color online) Radiated power from the first acoustic radiation mode.

FIG. 7. (Color online) Radiated power from the third acoustic radiation mode.

Table VIII. In Fig. 4, the primary force is denoted by f_p, the control force by f_c, and the error sensor locations by M_1, M_2, etc. It should be noted that the M_1 location is the location used previously.

As shown in Table VIII, locations M_1, M_2, M_3, M_6, and M_7 produced good results, while locations M_4 and M_5 produced a less desirable effect, leading to the notion that control is fairly independent of sensor location with the exception that error sensors should not be placed near the corners of the plate. This result is largely a function of using average values for α, β, γ, and δ over the entire frequency range. If the actual optimal values for α, β, γ, and δ are used for a specific mode, the overall attenuation is approximately equal to within less than 1 dB, no matter where the sensor is placed. However, since an average α, β, γ, and δ were selected, there are issues with placing sensors near corners. When placed in locations farther from the corners of the plate, the control of squared V_{comp} attenuated all of the peaks significantly and even provided control at frequencies other than the resonance frequencies. This result allows the sensor to be placed at a relatively arbitrary location, making this technique robust in terms of sensor placement.

C. Radiation mode comparison

A reason for the success of minimizing squared V_{comp} at certain modes and the lack of success by minimizing volume velocity is associated with the concept of acoustic radiation
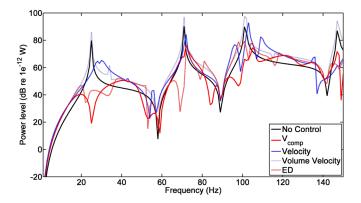
modes. The success lies in V_{comp}'s ability to control a number of acoustic radiation modes, as its terms mimic the first four radiation mode shapes. A comparison of the power radiated by the individual radiation modes, as given by Eq. (6), is shown in Figs. 5–8.

In comparing all of the cases, squared V_{comp} was the only control case which attenuated all of the peaks of the first four acoustic radiation modes. Energy density came close, but failed to control one of the peaks of the fourth radiation mode which corresponds to a frequency of 100 Hz, as can be seen in Fig. 8. As shown by Sors and Elliott,[8] volume velocity is a strong measure of the first acoustic radiation mode. When the first radiation mode has a strong response relative to the others, volume velocity control will perform well. Although volume velocity performed well overall, it did not attenuate any of the peaks for the even radiation modes as shown in Figs. 6 and 8. Squared V_{comp}, as a structural control metric, performs well in a broadband system because of its ability to control multiple acoustic radiation modes using a localized error measurement.

IV. CONCLUSIONS

This work has identified a new velocity-based objective function (squared V_{comp}) for ASAC. This objective function has been shown analytically to yield significant global attenuation of the acoustic radiation from a localized structural measurement.
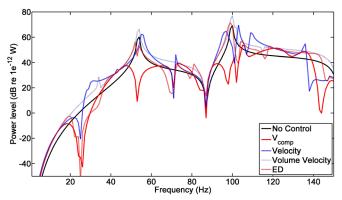

FIG. 6. (Color online) Radiated power from the second acoustic radiation mode.

FIG. 8. (Color online) Radiated power from the fourth acoustic radiation mode.

J. Acoust. Soc. Am., Vol. 131, No. 5, May 2012

J. M. Fisher et al.: Structural objective function   3839

To investigate various objective functions, a simply-supported plate was used as the base structure. In this investigation the quantity squared V_{comp} has emerged as an attractive quantity to approximate the ideal control objective quantity. It has been shown that V_{comp} is uniform over the surface of the plate when the weighting coefficients are properly chosen. Further, it has been shown that the terms in V_{comp} are closely related to the response associated with the first four acoustic radiation modes, which provides insight to the effectiveness of V_{comp} in minimizing acoustic radiation. Of the methods investigated, V_{comp} was the only method which provides attenuation for all peaks associated with the first four radiation modes. V_{comp} does require multiple velocity components, so multiple sensors are required, but those sensors are all localized to measure the response at a single location on the structure.

While these results are encouraging, further work is needed to investigate the effectiveness of this approach for more complex structures, such as ribbed plates, shells, etc. This is the focus of ongoing work.

ACKNOWLEDGMENT

[1]B. M. Faber and S. D. Sommerfeldt, "Global active control of energy density in a mock tractor cabin," Noise Control Eng. J. **54**, 187–193 (2006).

[2]S. D. Sommerfeldt and P. J. Nashif, "An adaptive filtered-x algorithm for energy-based active control," J. Acoust. Soc. Am. **96**, 300–306 (1994).

[3]C. R. Fuller, "Active control of sound transmission/radiation from elastic plates by vibration inputs: I. Analysis," J. Sound Vib. **136**, 1–15 (1990).

[4]C. R. Fuller, C. H. Hansen, and S. D. Snyder, "Active control of sound radiation from a vibrating rectangular panel by sound sources and vibration inputs: An experimental comparison," J. Sound Vib. **145**, 195–215 (1990).

[5]J. Pan, S. D. Snyder, and C. J. Hansen, "Active control of far-field sound radiated by a rectangular panel-A general analysis," J. Acoust. Soc. Am. **91**, 2056–2066 (1991).

[6]S. D. Snyder and N. Tanaka, "On feedforward active control of sound and vibration using vibration error signals," J. Acoust. Soc. Am. **94**, 2181–2193 (1993).

[7]S. D. Snyder and C. H. Hansen, "Mechanisms of active control by vibration sources," J. Sound Vib. **147**, 519–525 (1991).

[8]T. C. Sors and S. J. Elliott, "Volume velocity estimation with accelerometer arrays for active structural acoustic control," J. Sound Vib. **258**, 867–883 (2002).

[9]M. E. Johnson and S. J. Elliott, "Active control of sound radiation using volume velocity cancellation," J. Acoust. Soc. Am. **98**, 2174–2186 (1995).

[10]M. E. Johnson and S. J. Elliott, "Volume velocity sensors for active control," Proc. Inst. Acoust. **15**, 411–420 (1993).

[11]M. E. Johnson, "Active control of sound transmission," Ph.D. thesis, Institute of Sound and Vibration Research, University of Southampton, 1996.

[12]J. Rex and S. J. Elliott, "The QWSIS-a new sensor for structural radiation control," in *Proceedings of the First International Conference on Motion and Vibration Control*, Yokohama, Japan (1992), pp. 339–343.

[13]E. Johnson, T. Sors, S. J. Elliott, and B. Rafaely, "Feedback control of broadband sound radiation using a volume velocity sensor," in *Proceedings of Active'97*, Budapest, Hungary (1997), pp. 1007–1020.

[14]J. P. Maillard and C. R. Fuller, "Active control of sound radiation from cylinders with piezo-electric actuators and structural acoustic sensing," in *Proceedings of Active'97*, Budapest, Hungary (1997), pp. 1021–1034.

[15]J. P. Maillard and C. R. Fuller, "Advanced time domain wave-number sensing for structural acoustic systems. I: Theory and design," J. Acoust. Soc. Am. **95**, 3252–3261 (1994).

[16]J. P. Maillard and C. R. Fuller, "Advanced time domain wave-number sensing for structural acoustic systems. II: Active radiation control of a simply supported beam," J. Acoust. Soc. Am. **95**, 3262–3272 (1994).

[17]J. P. Maillard and C. R. Fuller, "Advanced time domain wave-number sensing for structural acoustic systems. III: Experiments on active broadband radiation control of a simply-supported pate," J. Acoust. Soc. Am. **98**, 2613–2621 (1995).

[18]N. Tanaka, S. D. Snyder, Y. Kikushima, and M. Kuroda, "Vortex structural power flow in a thin plate and the influence on the acoustic field," J. Acoust. Soc. Am. **96**, 1563–1574 (1994).

[19]S. D. Snyder, N. C. Brugan, and N. Tanaka, "An acoustic based modal filtering approach to sensing system design for active control of structural acoustic radiation: Theoretical development," Mech. Syst. Signal Process. **16**, 123–139 (2002).

[20]S. J. Elliott and M. E. Johnson, "Radiation modes and the active control of sound power," J. Acoust. Soc. Am. **94**, 2194–2204 (1993).

[21]K. A. Cunefare and M. N. Currey, "On the exterior acoustic radiation modes of structures," J. Acoust. Soc. Am. **96**, 2320–2312 (1996).

[22]C. Guigou, Z. Li, and C. R. Fuller, "The relationship between volume velocity and far-field radiated pressure of a planar structure," J. Sound Vib. **197**, 252–254 (1996).

[23]F. Fahy and P. Gardonio, *Sound and Structural Vibration: Radiation, Transmission and Response* (Elsevier, Oxford, 2007).